PERGAMON

Vision Research 40 (2000) 311–329

Vision Research

www.elsevier.com/locate/visres

Sensitivity to contrast modulation depends on carrier spatial frequency and orientation

Steven C. Dakin *, Isabelle Mareschal [1]

McGill Vision Research, Department of Ophthalmology, 687 Pine Avenue West H4-14, Montreal, Qué., Canada H3A 1A1

Received 18 May 1998; received in revised form 9 June 1999

Abstract

We consider how the detection of second-order contrast structure depends on the orientation and spatial frequency of first-order luminance structure. For patterns composed of a bandpass noise carrier multiplied by a contrast envelope function, we show that sensitivity to the envelope varies in proportion to the spatial frequency of the carrier. For oriented carriers at low spatial-frequencies, detection of the contrast envelope is easier when the envelope and carrier are perpendicular, but this dependency diminishes as the spatial frequency of the carrier increases. These differences are not attributable to either the detection of side-bands, or the presence of spurious contrast structure in unmodulated carrier images. A final experiment measured envelope detection in the presence of noise masks. Results indicate that orientationally and spatially-band pass filtering precedes the detection of second-order structure. © 2000 Elsevier Science Ltd. All rights reserved.

Keywords: Second-order; Orientation; Contrast; Texture

1. Introduction

Motivated by the work of Campbell and Robson (1968) many early models of low-level visual processing consist of linear filters selective for spatial frequency and orientation. Linear filters can reveal the presence of luminance-defined (or *first-order)* image structure, as indicated by their use in edge detection schemes (e.g. Marr & Hildreth, 1980). However, they cannot signal the presence of *second-order* structure that is defined by a change in higher-order image statistics such as local contrast or local orientation. The detection and discrimination of such stimuli requires that non-linear mechanisms be incorporated into models of early visual processing.

Contrast modulation (CM) has been the preferred class of second-order stimuli for psychophysical study (e.g. Burton, 1973; Henning, Hertz & Broadbent, 1975). Contrast modulated stimuli consist of a *carrier component* (often a sine-wave grating or noise texture) whose amplitude is modulated by an *envelope component*. Fig. 1a shows an example of such a stimulus, consisting of a horizontal, band-pass noise carrier whose contrast is modulated by a vertical Gabor function. Deriving regions of low and high contrast from this image (or *contrast demodulation)* cannot be achieved directly with linear filters[2]. A legitimate concern with respect to such stimuli is that these regions could be detected using a distortion product arising from a non-linearity preceding linear filtering (i.e. a small difference in the magnitude of responses to light and dark regions could introduce a weak first-order signal at the envelope spatial frequency). The bulk of psychophysical results does not support this hypothesis (Henning et al., 1975; Nachmias & Rogowitz, 1983; Derrington & Badcock, 1986; Cropper, 1998; Scott-Samuel & Georgeson, 1999).

* Corresponding author. Present address: Department of Visual Science, Institute of Ophthalmology, 11-43 Bath Street, London EC1V 9EL, UK. Fax: +44-171-608-6846.

E-mail address: s.dakin@ucl.ac.uk (S.C. Dakin)

[1] Present address: Center for Neural Science, New York University, 4 Washington Place, New York, NY 10003, USA.

[2] Strictly speaking because only contrast-modulated white noise is micro-balanced there may be first-order cues to the presence of the contrast structure in this image. The utility of such 'side-band' structure is considered in some detail below.

PII: S0042-6989(99)00179-0

Instead, the detection of second-order structure has suggested the existence of a non-linear processing stream that is generally thought to involve two filtering stages interposed by a non-linearity (referred to as a filter-rectify-filter (FRF) system; Fig. 1c and d; Chubb & Sperling, 1988; Sutter, Beck & Graham, 1989; Malik & Perona, 1990; Wilson, Ferrera & Yo, 1992). Recent physiological results suggest that the first-stage filters of the FRF system are located in cortex (Mareschal & Baker, 1998), and therefore band-pass in terms of both orientation and spatial frequency (Fig. 1d). In this paper we sought to investigate this psychophysically by examining how observers' detection of second-order structure depended on the spatial frequency and orientation content of the carrier.

Three issues bear on the properties of the notional FRF system. The first is the possibility that there is a single route to spatial form defined by all kinds of second-order structure, i.e. that contrast demodulation and texture segregation might be subserved by the same subprocesses. The second is that there is psychophysical evidence for a dependence of the detection of second-order structure on the range of spatial frequencies in the carrier, i.e. it is concerned with the *support* received by the second-stage filters from first-stage filters. The third is neurophysiological and psychophysical evidence pertaining directly to the *tuning* of the first-stage filters. We now review these issues in turn.

1.1. Single or multiple mechanisms for detecting second-order form?

It has long been known that two regions can be segmented based on their orientation content in the absence of a luminance discontinuity between them (Julesz, 1981; Beck, 1982) and that the strength of such segmentation depends primarily on the orientation difference between regions (Nothdurft, 1985). Discontinuities in orientation are one example of a *texture boundary*, which is also a second-order stimulus. Unsurprisingly then, many proposed texture segmentation algorithms have a filter-rectify-filter architecture of the sort described, with first stage local energy typically being the squared output of pairs of Gabor filters in quadrature phase (e.g. Fogel & Sagi, 1989; Bovik, Clark & Geisler, 1990; Malik & Perona, 1990). This energy representation is then processed with another linear filter bank in order to signal boundaries.

Fig. 1 illustrates how a FRF mechanism could be used to detect both texture- and contrast-defined structure. Both texture (including structure such as frequency modulation) and contrast boundaries lead to differential activation of a second-stage filter whose input is the rectified response of an oriented filter (Fig. 1d). In the motion domain, Ledgeway and Smith (1994) have similarly proposed that a FRF mechanism responding to the motion of contrast modulation could be used to signal other types of second-order motion (such as the motion of a modulation of carrier element size).

While detection of contrast boundaries and texture boundaries *could* be subserved by a common mechanism, orientation tuning of the first-stage filters depicted in Fig. 1d is not *required* for contrast demodulation. A filter receiving the rectified outputs of isotropic mechanisms (Fig. 1c) would operate just as effectively. In the following two sections we review direct evidence for the contrast demodulation system receiving input from mechanisms tuned for orientation and spatial frequency.

1.2. Support of second-stage filters: detection psychophysics

Jamar and Koenderink (1985) measured contrast modulation detection thresholds using two-dimensional white noise carriers whose contrast was sinusoidally modulated. They report that subjects' efficiency was equal irrespective of the bandwidth of the noise carrier, but was higher for high carrier spatial frequencies. They interpret these results as evidence for a second-order system receiving broad spatially tuned input. Sutter, Sperling and Chubb (1995) point out that Jamar and Koenderink's results could equally have arisen as a result of the visual systems' sensitivity varying asymmetrically around the centre frequency of carrier fre-

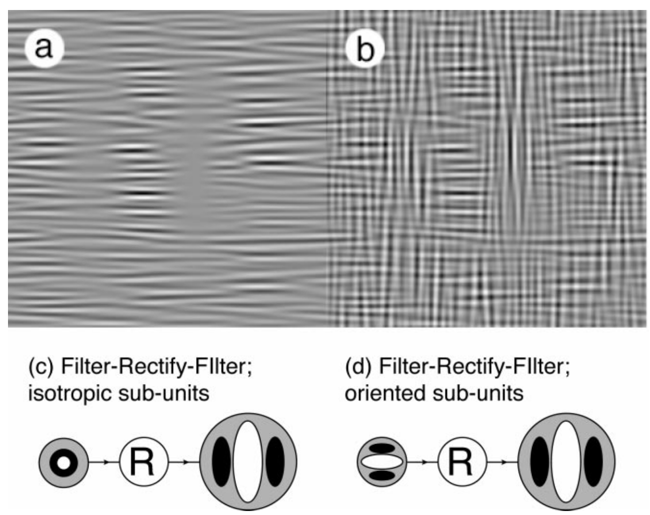

Fig. 1. (a) Horizontal noise carrier with contrast modulated by a vertical Gabor in sine phase. (b) Same image added to a vertical carrier modulated in sine + 180° phase. Detection of structure in (a) requires contrast demodulation and in (b) requires texture segregation. (c) Oriented second stage filters, operating on the rectified output of isotropic first-stage filters, signal the high-contrast regions of uniform orientation in (a) but not in (b). (d) A similar mechanism, using oriented first-stage filters, can signal both contrast structure and texture-defined structure.

quency bands tested. They measured CM thresholds as a function of the spatial frequency of the band-limited noise carriers employed. Sutter et al. report (shallow) band-pass tuning. However, Cropper (1998) found contrary results using sine-wave stimuli containing luminance and colour CM: he reports little or no effect of varying carrier spatial frequency within the range tested. The lack of consensus arising from these studies indicates that it is still unclear what carrier spatial frequencies support second-order processing at what envelope spatial frequencies.

Note that these studies measured CM detection thresholds either as a function of carrier spatial frequency or carrier bandwidth. However, although the above studies examined the possible range of first stage filter inputs, they did not examine the actual tuning of those mechanisms. The dependence of CM detection on carrier frequency could result either from (a) the broad tuning of the first-stage filters in the FRF system or (b) the pooled operation of a bank first-stage filters, narrowly tuned for both spatial frequency and orientation onto a second-stage filter. In the following sections we review evidence pertaining more directly to the tuning of first-stage mechanisms.

1.3. Tuning of first-stage filters

Langley, Fleet and Hibbard (1996) had subjects adapt to sine-wave gratings and then measured the resultant threshold elevation for detection of CM gratings. They report maximum threshold elevation (approximately a factor of 16) when the spatial frequency and orientation of the adapting grating matched the *carrier* rather than the *envelope* of the test pattern. This is consistent with the presence of orientationally and spatially-band pass filtering preceding the detection of second-order structure. It is interesting to note however that threshold elevation (of approximately a factor of 4) was observed even when the adapting stimulus was perpendicular to the carrier of the test stimulus. This indicates that orientational tuning of the first-stage filters may be broad.

Graham, Sutter and Venkatesan (1993) had subjects rate the strength of segregation between regions composed of Gabor micropatterns as a function of the difference in orientation and spatial frequency between elements comprising each region. Results were variable between subjects but generally indicated that first-stage filters are tuned for both spatial frequency and orientation although more broadly (around a factor of two) than channel estimates derived using texture differences based on first-order properties.

There is also neurophysiological evidence that neurons' responses to second-order structure are tuned to the carrier structure. Cells in the cat visual cortex respond to a static sine wave carrier whose contrast is modulated by a drifting low spatial frequency envelope (Zhou & Baker, 1993, 1994, 1996). The detection of these stimuli is contingent on the carrier frequencies falling within a narrow range of spatial frequencies. This work indicates that envelope responsive cells are tuned to a range of high carrier spatial frequencies (approximately 6–30 times the frequency of the envelope; Mareschal & Baker, 1998) with no evidence of a relationship between a cells' spatial frequency selectivity for the carrier and the envelope[3]. More recently, one of us (Mareschal & Baker, 1998, 1999) has found evidence that neurons' responses also display carrier *orientation* tuning, with no apparent fixed orientational relationship between the carrier and envelope processing stages. This endows neurons with the ability to respond not only to contrast modulation but also to various types of second-order structure (such as texture boundaries) in the way discussed above. That envelope responsive neurons are selective to the two-dimensional spatial characteristics of the carrier means that second-order processing is not occurring in the retina or LGN, but in the visual cortex.

To summarise, previous studies from adaptation and physiology have suggested that the operation of the second-order system may depend on the luminance-defined orientation and spatial frequency. Our goal is to determine the range of spatial frequencies/orientations that support the psychophysical detection of CM and to estimate the bandwidths of the filtering operations that subserve CM detection. In terms of the FRF model, we are asking which first-stage filters support which second-stage filters, and what are the spatial and orientational bandwidth of the first-stage filters[4]. Specifically, Experiments 2 and 3 investigate what luminance spatial frequencies and orientations support the detection of contrast structure at a particular CM spatial frequency. The results from these experiments provide estimates of the dependence of contrast demodulation performance on carrier structure but do not serve to identify the spatial and orientational bandwidth of *input* to the contrast demodulation system. To this end Experiment 4 considers the effects of noise masks on CM detection. Results provide direct psychophysical evidence that the mechanisms preceding CM

[3] That cells have been identified with a minimum 2.6 octave separation of preferred carrier and envelope spatial frequency is a consequence of a procedure which ensures that stimuli do not contain luminance components which fall within the cell's (luminance-defined) pass-band. When this constraint is relaxed envelope responsive cells have been found (in area MT of monkey) with closer carrier and envelope spatial frequency selectivity (O'Keefe and Movshon, 1998). However it is presently unclear if such results are an artefact of side-band Fourier structure falling into the cell's pass-band.

[4] The distinction between 'support from', and 'tuning of', first-stage filters was pointed out to us by an anonymous reviewer.

detection are tuned for both orientation and spatial frequency.

2. General methods

2.1. Subjects

The authors (SCD and IM) and two naïve subjects (HYW and RD) served as subjects in the experiments described. All wore optical correction as required and are experienced psychophysical subjects. They underwent a short training period, in order to familiarise themselves with the task, prior to threshold measurement. No significant effects of training were found in the course of the experiment.

2.2. Apparatus

An Apple Macintosh 7500 microcomputer controlled stimulus presentation and the recording of subjects' responses. Stimuli were displayed on a Nanao Flexscan 6600 monochrome monitor (frame refresh of 75 Hz) which was fitted with a video attenuator (ISR systems, Syracuse). Experiments were run from within the MatLab programming environment using display routines from the PsychToolbox (Brainard, 1997). A look-up table derived using the Videotoolbox package (Pelli, 1997) was used to linearise display luminance. Display linearity was further checked by changing viewing distance and ensuring that contrast modulation was only visible when the carrier was also visible. The screen was viewed at a distance of 62 cm and had a mean background luminance of 48 cd/m^2. SCD, IM and HYW viewed the screen binocularly, and RD viewed it monocularly. Monocular viewing produced little deterioration in performance for the conditions reported.

2.3. Stimuli: contrast modulation

The contrast of all stimuli was modulated by a Gabor function (offset by a d.c. term of 1.0); an isotropic Gaussian envelope multiplied by a sinusoidal grating. This function has the form:

$$G(x, y) = A\left[1 + \sin\left(\frac{x}{\lambda} + \phi\right)\exp\left(-\frac{x_t^2 + y_t^2}{2\sigma^2}\right)\right]$$

where A is the amplitude of the function (0.0–1.0), σ is the standard deviation of the Gaussian envelope (2 deg.), and λ the wavelength of the modulating sinusoid (2.82 deg.). x_t and y_t are co-ordinates rotated by 90°. This modulation function had a peak spatial frequency of approximately 0.35 cycles per degree (cpd). ϕ, the phase of the Gabor, was randomised (0–360°) from trial to trial so that the position of the low- and high-contrast regions of the carrier were also randomised. We used the same vertical, low-frequency contrast modulation function in all experiments reported here. Note that, although certain phases of the Gabor modulation have a small d.c. term and could conceivably introduce an 'overall' contrast cue, pilot studies indicated that this source of information did not significantly contribute to performance.

2.4. Stimuli: carrier images

For most stimuli, noise patterns were generated from 256 pixel-square white-noise textures containing a uniform random distribution of luminances. Filtering was performed in the Fourier domain and used idealised band-pass and orientation-limited kernels (i.e. sharp cut-off). Filters had spatial bandwidths of one octave and orientation information, when limited, was clipped in the range $\pm 10°$. Note that all spatial frequencies/orientations quoted for carrier images refer to the median of these uniform ranges (i.e. corresponding to the log-mean spatial frequency and the mean orientation). After filtering, images were normalised to a root mean square (RMS) contrast of 25% before storing off-line at 8 bit accuracy. Pixels with grey levels falling outside the permissible range were clipped.

Noise images generated in this way do contain elongated contrast structure that could potentially interact with the detectability of elongated contrast modulation structure. In a control condition to Experiment 3 we show that the magnitude of such effects proves to be quite small.

Stimuli were presented in the centre of the display and subtended 8 deg. square. Individual pixels were 1.9 arc min square. The highest frequency carrier condition, 16 cpd, required a frequency of 128 cycles per image (cpi) which is at the Nyquist limit for a 256 pixel square image. To accommodate this we used 512 pixel square images for this condition (where 16 cpd = 64 cpi), doubled the size of the Gabor modulation and also doubled the viewing distance accordingly. Unless stated otherwise, carriers were normalised to an RMS contrast of 25% prior to modulation. Examples of the stimuli are shown in Fig. 2.

2.5. Procedure

The experiment used a two-interval, two-alternative forced choice (2AFC) design. Subjects were sequentially presented with two different carrier images and were required to indicate in which interval was the carrier contrast modulated by the Gabor. This amounted to subjects detecting the presence of low and high contrast regions within the images. Stimuli were presented within a temporally sinusoidal (0.5 cycle) contrast window with a period of 1 s. The inter-stimulus interval was 500 ms.

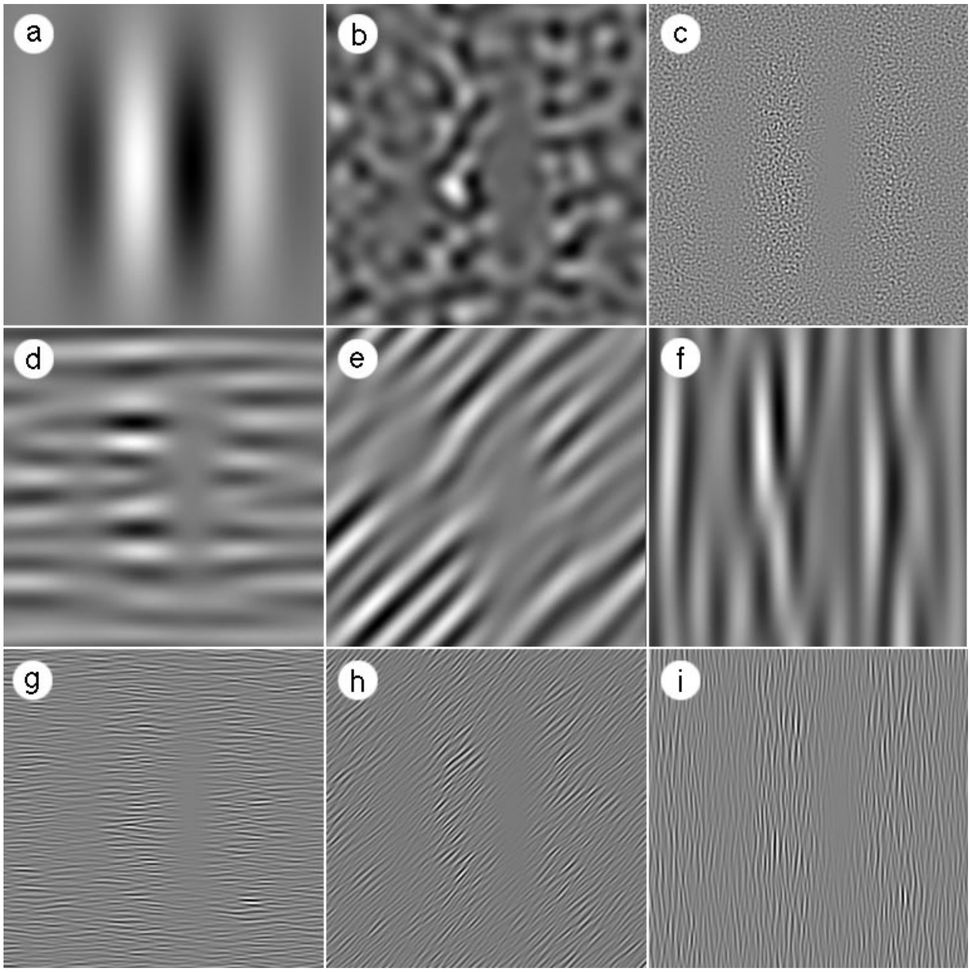

Fig. 2. (a) Typical Gabor function used to modulate the contrast of band-pass noise carriers. (b–i) Examples of the stimuli used in Experiments 1–3. Carriers have a mean spatial frequency (on log axes) of (b, d, e, f) 8 cpi and (c, g, h, i) 64 cpi, corresponding to 1 and 8 cpd at the viewing distance employed. Notice that the Gabor modulation is equally visible for all orientations of high frequency carrier (g–i) but is most visible with perpendicular low-frequency carriers (d).

Contrast modulation of the carrier was controlled by a 'one-up two-down' staircase method (Levitt, 1970), which terminated after ten reversals. The threshold from this procedure was the average of the last seven CM values producing reversals and is equivalent to 70.7% correct performance. Subsequently we refer to this threshold value, the minimum detectable depth of contrast modulation, as the 'CM threshold'. The values presented are the average of between three and six estimates of threshold, and error bars show ± 1 S.E.

Conditions were not interleaved, i.e. the only parameter varying within a block of runs was the depth of contrast modulation. Conditions were performed in a random order.

3. Experiment 1. The effect of carrier contrast on CM detection

Previously Jamar and co-workers (Jamar, Campagne & Koenderink, 1982; Jamar & Koenderink, 1985) measured the detectability of contrast modulation as a function of the contrast of a sine-wave grating carrier. They determined that increasing carrier contrast improves performance up to a level equivalent to about eight times (carrier) detection threshold. Beyond this point performance is constant. Cropper (1998) reports that the task becomes possible at contrasts around twice detection threshold, and that performance is largely unchanged beyond about five times detection threshold. In previous studies this pattern of results has not been seen to depend on carrier spatial frequency (Jamar et al., 1982; Jamar & Koenderink, 1985; Cropper, 1998)

In this experiment we sought to compare these results to CM detection with spatially bandpass noise carriers. This is necessary both to determine the possible role for side-bands in CM detection and to control for later conditions where carrier contrast is reduced in order to accommodate the contrast range occupied by noise masks. It is also interesting because, although noise carriers have been used previously to investigate the dependence of CM detection on luminance structure (Sutter et al., 1995), the effect of carrier visibility has not been assessed using band-pass noise carriers.

We measured detection of a vertical Gabor contrast modulation (0.35 cpd) using two carrier spatial frequencies (1.0 and 4.0 cpd) and three carrier orientations (isotropic, horizontal and vertical). In order that carriers should be equated for visibility we measured detection thresholds for each carrier and performed the CM detection at multiples of threshold carrier contrast. Detection thresholds for two subjects are shown in Table 1.

3.1. Results

The results from this experiment (plotted in Fig. 3) generally confirm the findings reported for beats and contrast modulated gratings (Jamar et al., 1982; Jamar & Koenderink, 1985; Cropper, 1998). Subjects show an initially strong dependence on carrier contrast and performance then levels off at supra-threshold levels. Notice that the point at which performance plateaus is typically around two to three times detection threshold for high-frequency isotropic carriers and slightly higher for the oriented carriers. For low frequency carriers, performance displays a shallower dependence on contrast than for carriers at higher spatial frequencies, with only a slight plateau at around four to five times detection threshold. A shallow dependence on carrier contrast is qualitatively similar to results reported by Cropper (1998) for all grating frequencies that he tested.

At low frequencies we note a large disadvantage for CM detection with vertical carriers at all contrast levels with performance being similar for isotropic and horizontal carriers. At high carrier frequencies (lower part of Fig. 3) performance with horizontal and vertical carriers is identical, being consistently worse than data from the isotropic carrier condition. This dependency of CM detection on carrier spatial frequency and orientation is investigated in more detail in the next experiment.

Table 1
Detection thresholds (% contrast) for isotropic, horizontal and vertical carriers at two spatial frequencies[a]

	Isotropic	Horizontal	Vertical
SCD (1 cpd)	1.53 (0 07)	1.04 (0.08)	1.0 (0.16)
SCD (4 cpd)	2.25 (0.15)	1.06 (0.03)	1.3 (0.15)
HYW (1 cpd)	1.49 (0.08)	1.18 (0.20)	1.10 (0.13)
HYW (4 cpd)	2.63 (0.31)	1.71 (0.12)	1.70 (0.11)

[a] Figures in brackets are estimated standard errors.

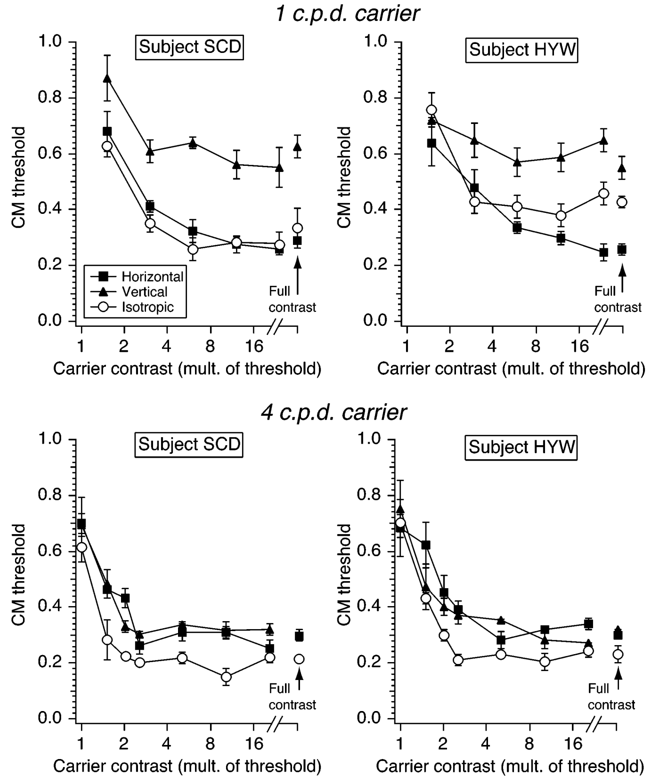

Fig. 3. Results from Experiment 1: the effect of carrier contrast on CM detection, for horizontal, vertical and isotropic carriers at two spatial frequencies. Graphs show the depth of contrast modulation (corresponding to parameter A in Equation 1) detectable at threshold (70.7%) as a function of the contrast of the carrier (expressed in multiples of detection threshold).

4. Experiment 2. The effect of carrier spatial frequency on CM detection

Results from the previous experiment suggest that the spatial frequency and orientation of the carrier affect observers' sensitivity to contrast modulation. Previously, Sutter et al. (1995) reported that sensitivity to contrast modulation is a band-pass function of carrier spatial frequency, for isotropic noise carriers. We sought to confirm this result because different results have been reported with sine-wave carriers (e.g. Cropper, 1998). Also, given that first-stage filters are thought to be oriented, we wished to determine if the observed tuning for isotropic carriers would be similar for CM thresholds measured with oriented carriers. (One might expect this to be so if the second-order filtering system equally weights the rectified output of the filters that form its input.)

We measured the detectability of a 0.35 cpd vertical Gabor contrast modulation with noise carriers at 0.7, 1.0, 1.4, 2.0, 2.8, 4.0, and 8.0 cpd. Carriers were either isotropic or limited ($\pm 10°$) to either horizontal or vertical orientations. Carrier contrast was maximised (RMS contrast 25%) so as to accommodate a 100%

contrast modulation. Examples of the stimuli are shown in Fig. 2.

4.1. Control condition: the role of side-band structure in CM detection using noise carriers

Although the use of high-contrast carriers is prevalent in the second-order literature, their use both exacerbates and highlights two problems with the use of contrast modulated stimuli: the presence of side-band structure (Henning et al., 1975) and 'spurious' contrast structure (Kovacs & Feher, 1997). Control conditions were run to assess the effects of these two types of spatial structure on our task. Here we describe the control condition for sideband structure and in Experiment 3 we describe the control condition for spurious contrast structure.

Contrast modulation of a sine-wave grating introduces energy into so-called 'side-band' spatial frequencies. The magnitude of these side-band components depends on the similarity between the spatial frequency of carrier and envelope (Fig. 4). The extent to which these components play a role in CM detection determines the truth of Campbell and Robson's (1968) proposition that the visual system operates as a bank of independent linear filters. If such side-band components are all that are available to signal CM then modulation should be signalled only when the energy in one of these side-bands exceeds the contrast threshold of a filter tuned to the side-band spatial frequency. Henning et al. (1975) used contrast modulated, low-contrast (6%) grating carriers to show that modulation detection thresholds are actually about a third what would be predicted using such a scheme. Jamar et al. (1982), using frequency modulated gratings (which they equated to CM data by matching side-band energy), determined that the importance of side-bands depends on carrier contrast. At low contrasts the independent filters scheme is a poor predictor of performance, but improves as carriers become strongly supra-threshold. Although the balance of evidence suggests that side-band information is useful for high contrast carriers, this is rarely considered in the second-order literature even though the use of high-contrast carriers is widespread.

To test the assumption of complete channel independence Henning et al. (1975) measured side band detectability *in the absence of the carrier*. That is, stimuli consisted of two superimposed gratings at the frequency of the side-bands in the original CM patterns. This is a strong test of the contribution of side-bands; for a real CM detection task the side-bands are accompanied by high energy carrier structure which is (by definition) in nearby spatial frequency bands and could serve to mask side-band detection. Because we were interested in assessing the role of side-band information

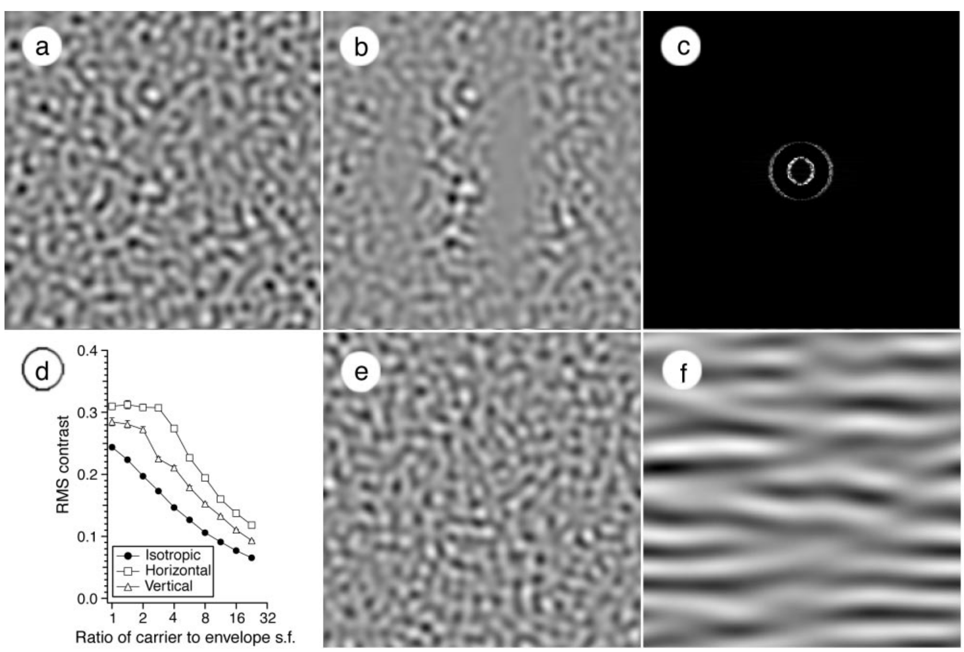

Fig. 4. (a) An isotropic carrier at 16 cpi (2 cpd in our experiment), (b) contrast modulation by a vertical Gabor introduces spurious 'side band' power, shown in (c) as a power plot. (d) The contrast energy of this structure depends on how similar carrier and envelope are in spatial frequency and how dissimilar in orientation. The graph shows side-band contrast energy for a 100% contrast modulated pattern; notice that side-band energy is around 15% for an isotropic carrier even when carrier and envelope are separated by a fourfold ratio of spatial frequency. (e) Phase randomised version of (b). This has the same side-band structure as (b) but, in terms of its wider bandwidth, is not discriminable from (a). (f) Phase randomised version of Fig. 2d. For low-frequency horizontal carriers side-band energy is visible as discontinuities in the orientation structure ('kinks' in the bright and dark blobs).

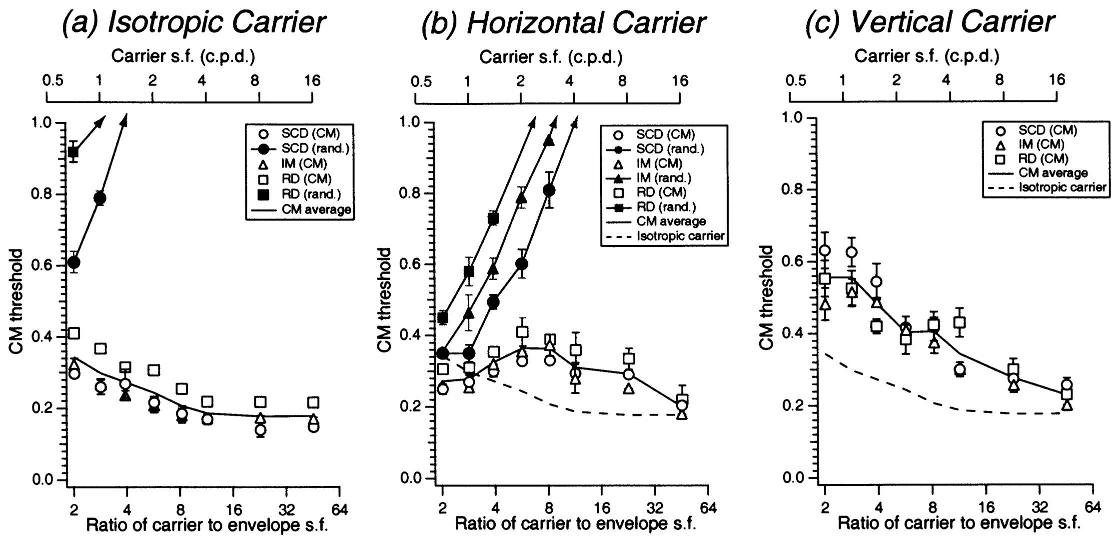

Fig. 5. Results from Experiment 2. Unfilled symbols show contrast modulation thresholds (the minimum detectable CM depth) as a function of the ratio of carrier to envelope spatial frequency for (a) isotropic, (b) horizontal and (c) vertical carriers. Solid lines show thresholds averaged across the three observers. Filled symbols indicate discrimination of phase randomised CM stimuli, when subjects performed the task based only on the energy that is introduced into 'side-band' spatial frequencies by the modulation procedure. (Although we tested the same range of carrier spatial frequencies, data are presented only when thresholds were measurable.)

in observers performing our CM detection task but were not interested in testing channel independence *per se*, we devised a novel control task. Contrast modulation information for an image is captured primarily by the phase spectrum; it is not possible to deduce the contrast structure of an image based on the distribution of energy in the amplitude domain. As the spatial frequency of carrier and envelope approach one another the energy at side-band spatial frequencies increases. If CM detection is performed from such first-order artifacts one should be able to discriminate a carrier image from a contrast-modulated carrier that had been phase-randomised. The latter (examples are shown in Fig. 4e–f) has identical side-band energy to the contrast-modulated pattern. Thus, our first control experiment was identical to the main condition — we measured a CM threshold using the same procedure — but contrast-modulated images were phase-randomised prior to presentation. Subjects indicated which interval contained the carrier with the broader bandwidth (where each interval employed a different carrier image). This manipulation allows us to assess whether subjects detect contrast modulation using side-band structure or if it is the spatial pattern of contrast in the pattern that is useful. Phase randomisation was performed in the Fourier domain. Images were forward Fourier transformed and separated into amplitude and phase components. The amplitude components were retained but the phase components were replaced with angles selected, using a uniform random distribution, from the interval 0 to 360°. The angles used maintained global Hermitian symmetry ensuring that the back-transform would contain no imaginary components. Images were then reverse transformed. Note that because phase-scrambled images have identical power spectra to their contrast modulated counterparts they will also have identical RMS contrast.

4.2. Results

Fig. 5 shows CM detection thresholds as a function of the ratio of the spatial frequency of isotropic, horizontal and vertical carriers to the spatial frequency of the envelope. The steady reduction in threshold with increasing frequency of isotropic carriers (Fig. 5a) is consistent with results from Jamar and Koenderink (1985), which they interpret as evidence for broadband tuning of the first-stage filters, and from Cropper (1998). Our data are also qualitatively similar to results reported by Sutter et al. (1995) although they also report a slight deterioration in performance at very high ratios of carrier to envelope spatial frequencies (32:1).

Fig. 5b and c show the carrier spatial-frequency tuning obtained with horizontal and vertical carriers. First note that curves are substantially different to those shown in Fig. 5a. Tuning for horizontal carriers is shallower and, if anything, implicates an underlying mechanism with somewhat band-reject characteristics. Performance with the horizontal carriers exceeds performance with isotropic carriers at low spatial frequencies, but this pattern reverses at a carrier to envelope s.f. ratio of around 4:1 (i.e. a carrier spatial frequency of about 1.1 cpd). Beyond this point results with horizontal carriers are consistently worse than with isotropic carriers. Results for the vertical carriers are quite different: thresholds are consistently higher than data for isotropic carriers. From Fig. 5b and c note that performance with oriented carriers (unfilled symbols) is slower to improve as a function of carrier spatial frequency than isotropic carriers (dashed lines). We return to this point in Experiment 3.

The filled symbols in Fig. 5 show results from the control experiment where subjects discriminated phase-randomised versions of the CM stimuli from unmodulated carrier images. None of the subjects could perform the discrimination with vertical carriers, where the presence of the side-band information was completely masked by the carrier. Similarly for the isotropic carrier, only a narrow range of low frequency carriers produced discriminable side-band structure. Of the three carrier types tested, horizontal carriers introduced side-band structure that was discriminable over the widest range of ratios of envelope to carrier spatial frequencies. Perceptually, side-bands produce 'kinks' in the orientation structure that is discriminable from the appearance of the original carrier (e.g. Fig. 2i). However in all cases detection thresholds for the phase-randomised stimuli exceed those observed with the normal CM stimuli. For very low frequency perpendicular carriers their role cannot be discounted but these data make it unlikely that side-band detection *in isolation* is responsible for the CM detection results observed. If first-order artifacts are being used in this task they must be being combined with second-order information about the CM structure.

The monotonic dependence of CM threshold on the spatial frequency of an isotropic carrier (Fig. 5a) argues against preferred carrier spatial frequencies for CM detection at a particular CM frequency. In terms of the FRF model it argues against a fixed relationship between the peak spatial frequency preference of first- and second-stage filters. In order to determine the generality of this finding we varied the spatial frequency of the CM itself. We reran two subjects on the isotropic carrier condition but in this case similar stimuli were viewed at twice the viewing distance (124 cm) doubling the spatial frequency of both envelope and carrier. Results are plotted in Fig. 6 and show the same proportional relationship between ratio of carrier to envelope spatial frequency and CM threshold. The close correspondence between data measured at the two viewing distances indicates that this task exhibits *scale invariance* so that it is reasonable to assume that CM detection shows a monotonic dependence on the ratio of carrier to envelope spatial frequency regardless of absolute envelope spatial frequency.

5. Experiment 3. The effect of carrier orientation on CM detection

Fig. 7 is a replot of data from Fig. 5, showing the ratio of thresholds for horizontal and vertical carriers at the same spatial frequency. Notice that the data indicate equal performance at ratios of carrier to envelope spatial frequencies above approximately 11:1. This suggests orientational tuning changes with spatial frequency. To investigate this further we measured CM thresholds at four carrier spatial frequencies (1, 2, 4 and 8 cpd), and nine carrier orientations (0, 15, 30, 45, 60, 75, 80, 85 and 90°). Contrast modulation was again fixed at 0.35 cpd, and 90°.

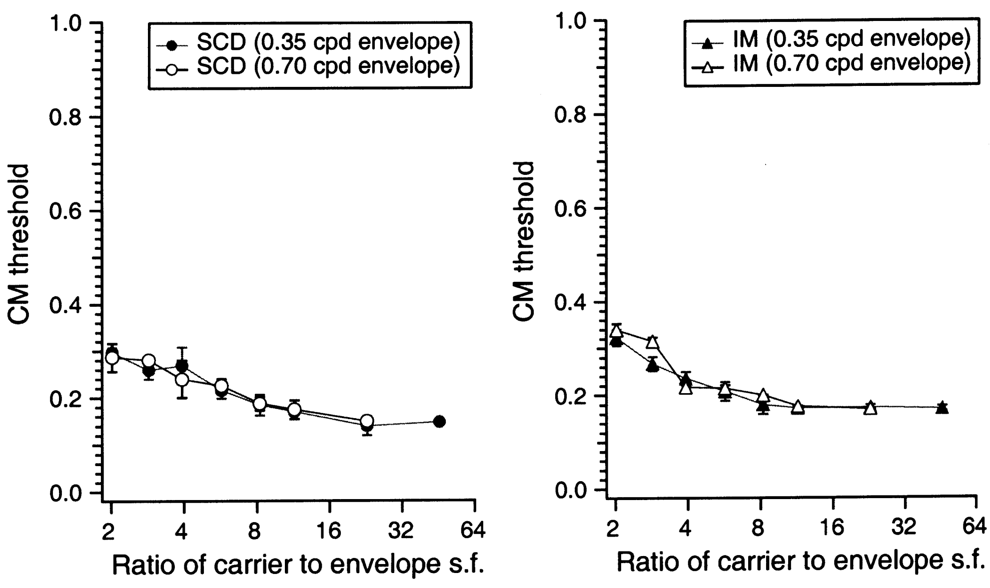

Fig. 6. CM detection as a function of the ratio of the spatial frequency of carrier to envelope for isotropic carriers. The two graphs show data from two subjects, open and closed symbols are data measured at two viewing distances. Performance shows little dependence on viewing distance and we observe the same monotonic dependence of threshold on ratio of carrier to envelope spatial frequency.

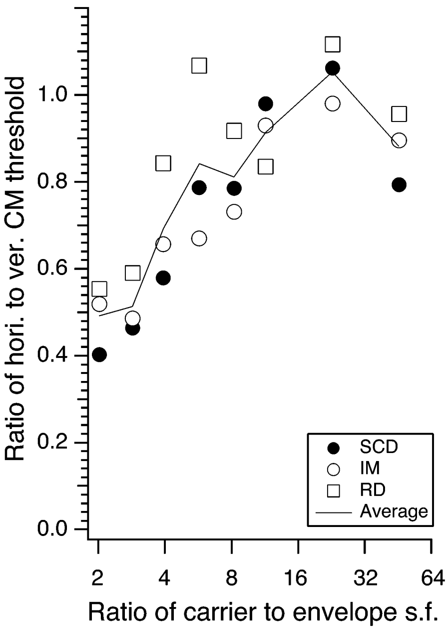

Fig. 7. Ratio of CM thresholds with horizontal carriers to thresholds with vertical carriers as a function of the ratio of carrier to envelope spatial frequency. Symbol type indicates data from the three subjects. Tuning approaches isotropy for ratios of carrier to envelope spatial frequency exceeding around 11:1.

Fig. 8 shows results from two subjects for this condition, with solid lines indicating performance averaged across the subjects. For the two lowest frequencies tested (a and b) subjects are most sensitive at detecting a vertical CM with carriers around horizontal. Performance decreases as the carrier approaches envelope orientation with a pronounced 'notch' around 75° (for the 1 cpd carrier) and 80° (for the 2 cpd carrier). Subjectively, this pattern of results has two components: an improvement at around 15° and a deterioration at 30°. From inspection of the patterns this would seem to be due to a contribution from elongated contrast structure that arises by chance in carrier images prior to modulation. The observed improvement could be due to this structure reinforcing the contrast structure of the CM patch, and the deterioration to it masking detection of the CM patch. This would be consistent with the fact that such contrast structure tends to arise at orientations near the orientation cut-off for the noise ($\pm 10°$). We return to the role of spurious carrier contrast structure in the following control condition. Notice that the degree of tuning is reduced going from a 1–2 cpd carrier. This trend continues with results for the two higher frequencies indicating little or no tuning to the carrier orientation.

These results indicate that CM detection shows a decreasing dependence on carrier orientation as carrier spatial frequency increases. This could provide an explanation for our earlier observation that CM detection plateaus at lower spatial frequencies with isotropic carriers than with oriented carriers (compare unfilled symbols and dashed lines in Fig. 5b and c). It may be that the visual system integrates over a wider range of orientations at higher carrier spatial frequencies. This integration could be achieved at the level of first-stage filters (by making them broader bandwidth) or at the level of second-stage filters (by allowing them to integrate over a wider range of narrowly-tuned first-stage filters). We return to the problem of determining the site of this integration in Experiment 4.

5.1. Control condition: the role of spurious carrier contrast structure in CM detection

Consider Fig. 9a which depicts a typical oriented carrier image used in the experiments described so far. Kovacs and Feher (1997) point out that such spatially band-pass noise images contain 'spurious' second-order structure, visible as a 'web' of low contrast regions throughout the image. It is clear that the orientation and spatial frequency of such structure is related to that of the carrier. To address if this structure could be determining performance in the experiments reported we reran Experiment 2 using stimuli which had been pre-processed to 'flatten' such contrast structure (e.g. Fig. 9b) using the method described in Kovacs and Feher (1997). The reader is referred to the original paper for a full description of the technique but, in brief, it involves estimation of local contrast by computing the range of intensities local to each point in an image. The original image is then divided by a smoothed version of this representation. Provided the circular neighbourhood over which local contrast estimation and smoothing occurs is sufficiently large (compared to the wavelength of the noise) then the spatial frequency structure of the noise remains largely unaltered but the amplitude of spurious contrast modulation is minimised. We follow Kovacs and Feher (1997) in using a neighbourhood radius equal to twice the wavelength of the noise.

5.2. Results

Fig. 10 shows data from the 'flattened contrast' carrier condition for the two lowest spatial frequencies tested. Notice that the notches around 15° in the tuning function for 1 cpd carriers are greatly reduced but that the magnitude of the data is closely consistent with the data collected using normal noise carriers. This confirms that the reduction in threshold at orientations near the edge of low-frequency carriers' orientational pass-band, observed in Experiment 2, is due to a contrast pedestal effect arising from spurious contrast structure in the carrier. It also indicates that the elevation of thresholds at carrier-envelope orientation differences of around 30° is due to masking of the CM patch by spurious carrier contrast. That the overall pattern of results is largely unchanged, however, suggests that spurious contrast structure in the carrier plays only a minor role in determining underlying tuning of CM detection to carrier structure at all other carrier orientations. For this reason we did not feel it was necessary to use 'flattened contrast' noise carriers in the experiments which follow.

6. Experiment 4. Dependence of CM detection on carrier structure assessed with noise masking

The results reported so far are consistent with the contrast demodulation system receiving spatially broad-band input with orientation band-width increasing with spatial frequency. Observers' performance generally improves with the spatial frequency of the carrier and their superior performance with isotropic carriers suggests that this could be due to pooling of information across carrier orientation. However, note that these data bear only on the *support* the second-order system receives from first-stage mechanisms. They do not constrain the form of the first-stage filters themselves. For example, a FRF system with isotropic first-stage input (e.g. Fig. 1c) would demodulate the contrast component of all stimuli employed so far, just as effectively as one employing oriented first-stage filters (e.g. Fig. 1d). The use of oriented carriers does not require that the visual system apply an oriented mechanism to detect

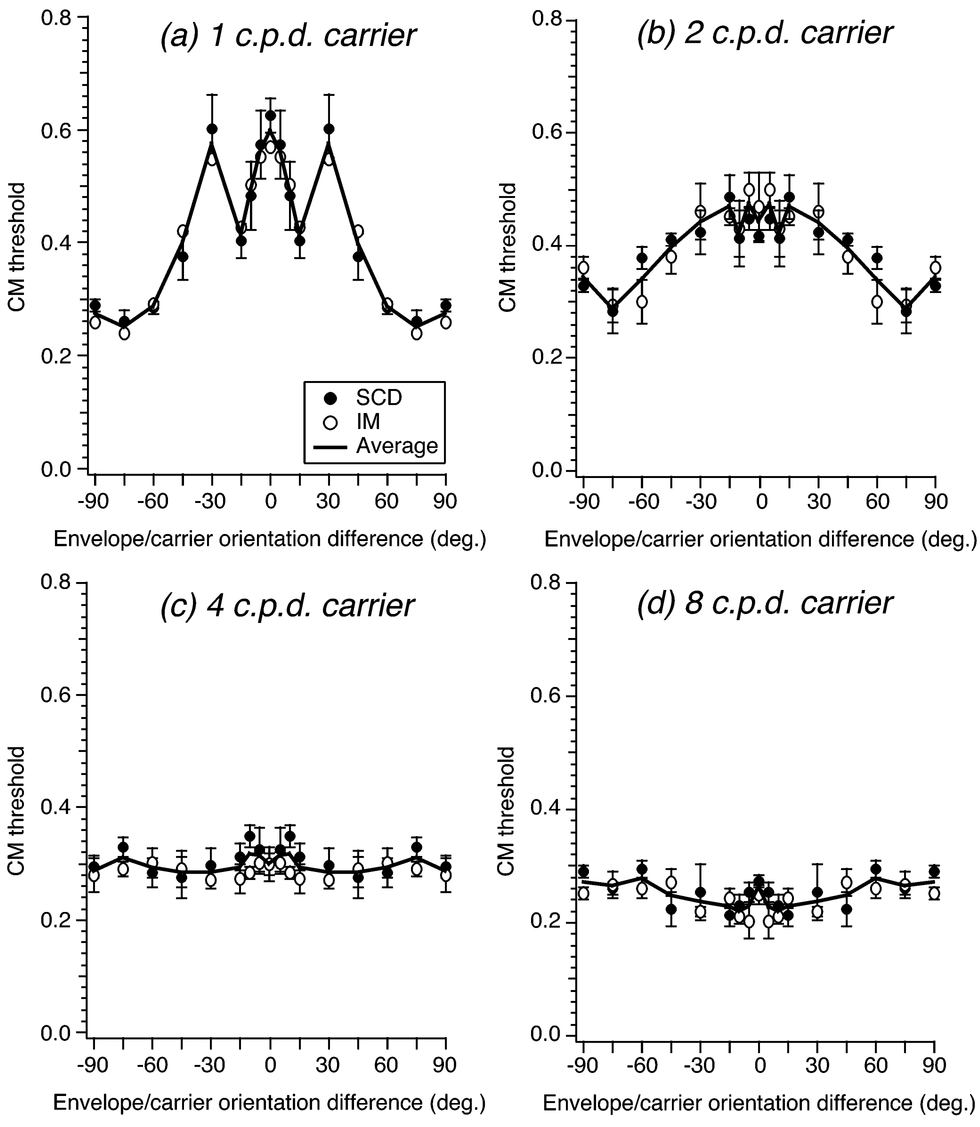

Fig. 8. Results from Experiment 3. Contrast modulation thresholds as a function of carrier orientation for carrier spatial frequencies of (a–d) 1–8 cpd. Data have been reflected around the 0° axis. At low carrier spatial frequencies (a and b) subjects are most sensitive to CM structure oriented perpendicular to the carrier. Note also the 'notches' in the tuning function for carrier/envelope difference of 30°; this is likely to be due to spurious contrast structure in the carrier. At higher frequencies (c and d) carrier orientation preference is greatly reduced.

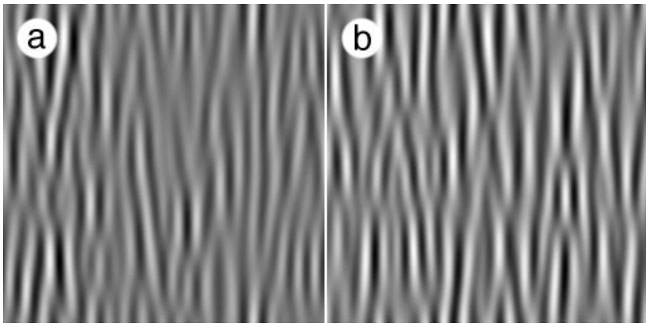

Fig. 9. (a) Vertical carrier image with a mean spatial frequency of 16 cpi (2 cpd in the experiment). Note the spatially 'uneven' contrast. (b) A carrier at the same spatial frequency after 'contrast flattening' to reduce spurious contrast variation. This procedure does not significantly alter the power spectrum of the image.

contrast modulation. Indeed, the hypothesis that first-stage filters are broad-band has a significant computational advantage over a system employing narrow-band first-stage filters; it requires many fewer filters. This problem of filter proliferation in FRF schemes has been observed previously (Wilson & Richards, 1992). However, it would seem to be unavoidable if one is to retain the selectivity of second-stage filters for their first-stage sub-units. As we observed in the Introduction (see Fig. 1) this is a necessary condition for a single second-order system to subserve both the detection of contrast- and texture-defined form. We return to this point in Section 7.

If the first-stage filters are broad-band (either in orientation or spatial frequency) first-order structure is collapsed across orientation or spatial frequency before the visual system attempts to infer the presence of contrast structure. Therefore the presence of irrelevant first-order structure in the pattern cannot be ignored. From this point of view, the simplest form of irrelevant structure is unmodulated luminance information that will serve to reduce the strength of the contrast signal reaching the second-stage filters. On the other hand, if the first-stage filters are tuned, the contrast demodulation system should be able to ignore unmodulated first-order structure when it falls beyond the sensitivity of the filter in question.

We tested these two theories directly using a masking paradigm; we measured CM detection in the presence of unmodulated noise images. The hypothesis that first-stage filters are broad-band predicts that the presence of unmodulated luminance structure will have a detrimental effect on CM detection irrespective of the relationship of the mask to carrier (either in terms of orientation or spatial frequency). The presence of narrow-band first-stage filters predicts that the disruptive effect of the mask will depend on the similarity of mask and carrier in terms of orientation and/or spatial frequency.

For the spatial frequency condition we measured CM detection thresholds using isotropic carriers at 2.8 cpd (with an RMS contrast of 12.5%), in the presence of a contrast mask which consisted of an unmodulated spatially bandpass noise image. We used carriers with an RMS contrast of 12.5% so that full amplitude modulation would fill half the permissible range of grey-levels (leaving the other half for the mask). We then systematically varied the spatial frequency of the mask image from 0.71 to 11.3 cpd. For the orientation condition we used 12.5% RMS contrast carriers at 4 cpd and at

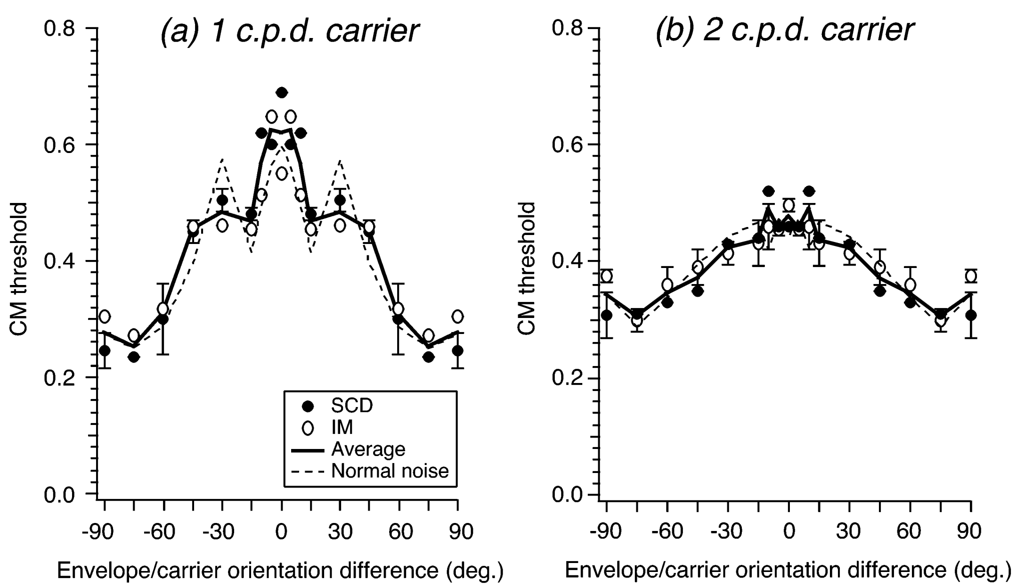

Fig. 10. CM thresholds for carriers with 'flattened contrast' at (a) 1.0 cpd and (b) 2.0 cpd as a function of carrier orientation. Solid lines again indicate performance averaged across the two observers. Tuning is similar to that observed in Experiment 1 except for the absence of notches around 15° carrier/envelope orientation differences.

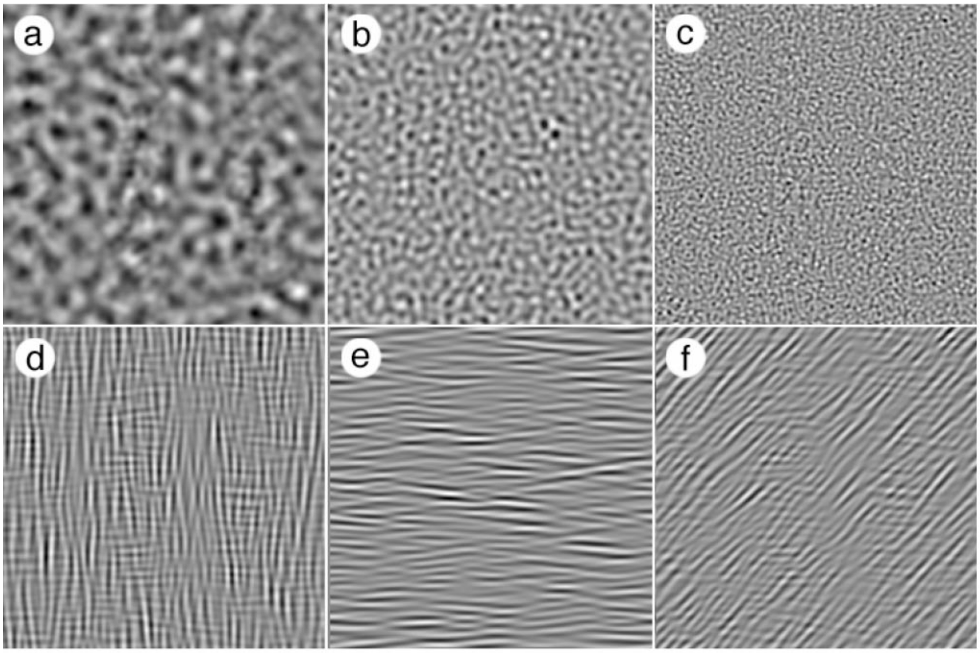

Fig. 11. Stimuli contain a vertical contrast modulation at 0.35 cpd, with an unmodulated masking noise image superimposed. (a–c) 2.8 cpd isotropic carrier with a 50% contrast isotropic mask added at (a) 1.4 cpd (b) 2.8 cpd and (c) 5.6 cpd (d–f) Horizontal 4.0 cpd carrier with a 4.0 cpd mask at (d) 90°, (e) 0° and (f) 45°.

either 0, 22.5, 45 or 90°. A slightly higher carrier frequency was used in this condition to ensure that any absolute differences in performance between carrier orientations were minimised (see Experiment 2). The masks used in the orientation condition were orientationally band-limited noise images at the same spatial frequency as the carrier and were varied from −75 to 90° in 15° steps. Note that in all conditions we again used the same 0.35 cpd vertical contrast modulation. Fig. 11 shows examples of the stimuli used in (top row) the spatial frequency condition and (bottom row) the orientation condition.

6.1. Results

Fig. 12 shows CM detection accuracy, for a 2.8 cpd isotropic carrier modulated by a vertical 0.35 cpd Gabor, as a function of the ratio of the spatial fre-

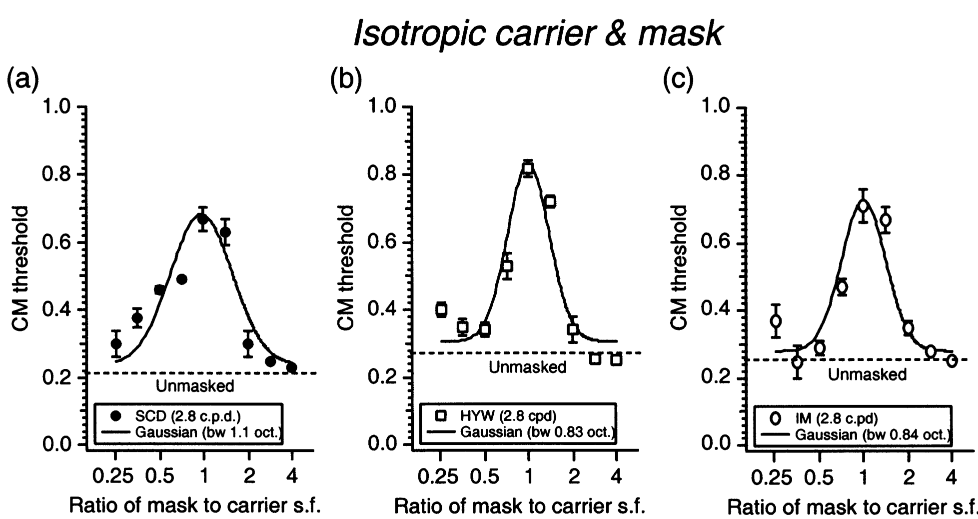

Fig. 12. Results from Experiment 4: CM detection thresholds (isotropic carrier) as a function of the ratio of mask to carrier spatial frequency. Data show clear band-pass tuning, and are fit by log Gaussians.

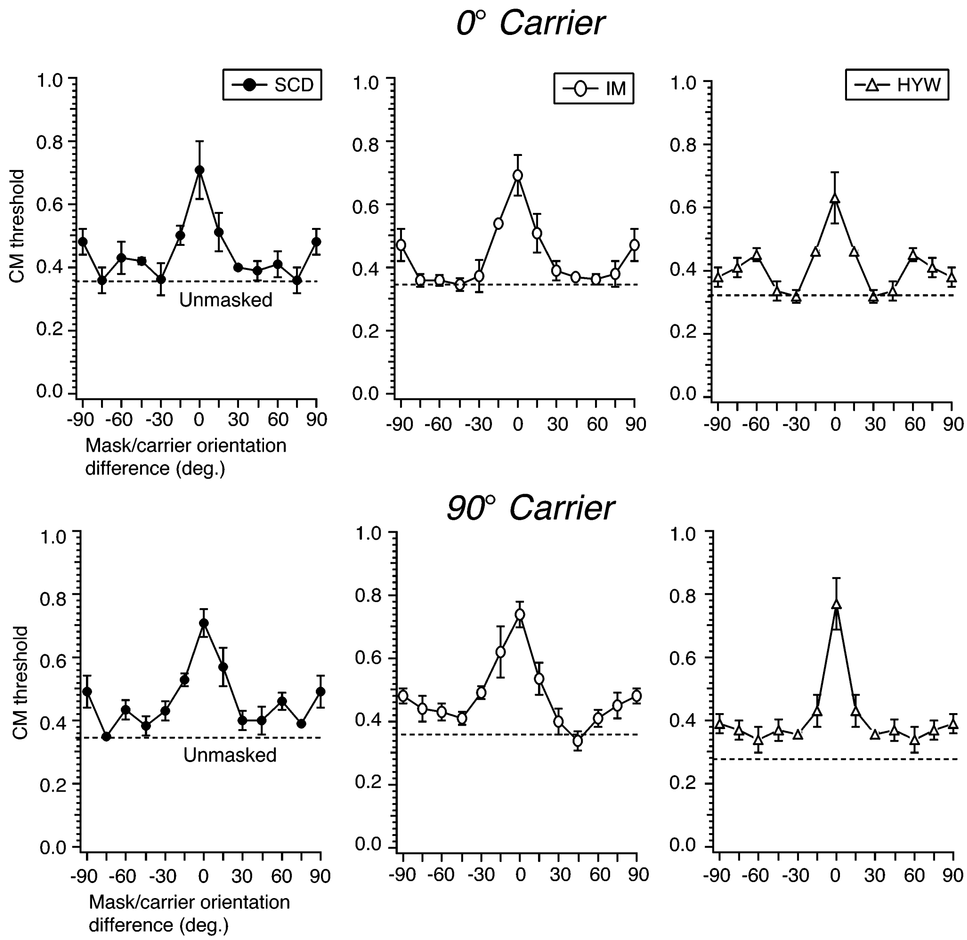

Fig. 13. CM detection with horizontal and vertical noise carriers as a function of the difference between carrier and mask orientation. A positive orientation difference indicates the mask was anti-clockwise from the carrier. Notice that peak masking occurs when the masking image matches the orientation of the carrier. There is also a suggestion of a second peak in the tuning functions when the mask is *perpendicular* to the carrier. Data from HYW (the rightmost plots) have been reflected around the 0° point on the abscissa.

quency of an isotropic mask image to the spatial frequency of the carrier. The dashed line indicates unmasked CM detection thresholds. Performance is clearly elevated in the presence of a mask and indicates band-pass tuning of CM detection for carrier spatial frequency. Notice that although data are reasonably well fit by a log-Gaussian, tuning is not precisely symmetrical on log-axes (Solomon & Watson, 1995). A noise image which is an octave higher in spatial frequency than the carrier is a more effective mask for CM detection than the equivalent mask at a spatial frequency one octave lower. Also low spatial frequency masks seem to show a slightly shallower roll-off. The half-width at half-height bandwidths for the data shown are 1.1 octaves (SCD), 0.83 octaves (HYW) and 0.84 octaves (IM). These values are in accord with previously reported psychophysical estimates of channel bandwidth (around 0.5–1.25 octaves) derived using a number of techniques such as masking (Legge & Foley, 1980; Henning, Hertz & Hinton, 1981; Wilson, McFarlane & Phillips, 1983) and spatial summation (Mostafavi & Sakrison, 1976; Watson, 1982).

The effect of mask orientation on CM detection is plotted in Fig. 13. CM detection thresholds are shown as a function of the difference in orientation between carrier and mask, for horizontal and vertical carriers. Threshold elevation is greatest when masks are matched to the orientation of the carrier, and indicate

Table 2
Half-width at half-height orientation bandwidths for tuning of CM detection assessed using masking

Subject	0° carrier (°)	22.5° carrier (°)	45° carrier	90° carrier
SCD	15.6	22.5	29.8	20.0
IM	16.3	20.4	33.5	17.5
HYW	12.2	34.7	32.4	12.7

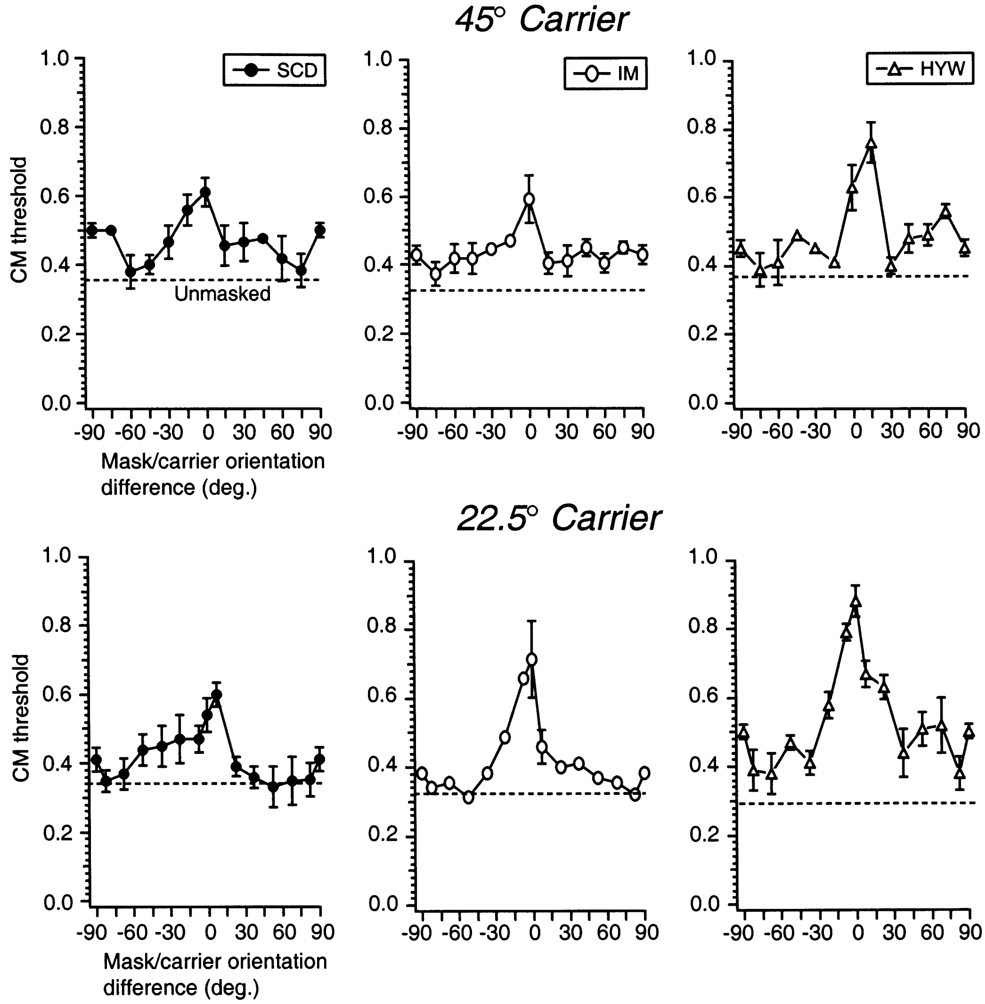

Fig. 14. CM detection with oblique noise carriers (45 and 22.5° anti-clockwise from horizontal) as a function of the difference between mask and carrier orientation. Recall that a positively signed difference means the mask was anti-clockwise of the carrier.

band-pass tuning with respect to carrier orientation. When mask and carrier differ by more than around 30° little masking is observed although all subjects show marginal elevation of thresholds when carrier and envelope are perpendicular. The magnitude of this effect is small for subject HYW and in part this seems to be due to his showing some threshold elevation irrespective of mask orientation (general elevation of tuning function above unmasked detection thresholds in lower right part of Fig. 13). The presence of notches in our orientation tuning functions around 45° is qualitatively similar to psychophysical results presented by Ringach (1998) and to the more general notion of inter-orientation inhibition (e.g. Andrews, 1965; Blakemore & Carpenter, 1970).

Estimates of orientation bandwidth for this condition are given in Table 2 (first and last columns). These estimates are based on a Gaussian fit to the data, where the d.c. level of the function is fixed at the unmasked CM detection threshold. This effectively removes the influence of the threshold elevation at orthogonal mask-carrier combinations. Values average about 15° which is consistent with estimates of orientation bandwidth derived using various psychophysical (e.g. Mostafavi & Sakrison, 1976; Phillips & Wilson, 1983; Dannemiller & Ver Hoeve, 1990) and neurophysiological techniques (Daugman, 1985).

Fig. 14 shows tuning derived using carriers at 45 and 22.5°. First note that tuning is less symmetrical than for the corresponding conditions shown in the last figure. There is a tendency (five of the six conditions shown) for masks oriented near to horizontal to be more effective than those near to vertical. Also, all subjects show generally greater vulnerability to masks with oblique carriers compared to horizontal and vertical carriers (compare tuning functions for subject IM with horizontal and 45° carriers). Performance does not so sharply approach unmasked levels with oblique carriers and this is reflected in the broader bandwidth estimates given in Table 2. Whether mechanisms tuned to oblique orientations are more broadly tuned is contentious (e.g. Thomas & Gille, 1979; Harvey & Doan, 1990) but it is important to note that the increase in bandwidth we report is accompanied by, and largely due to, increasing *asymmetry* in the data.

7. Discussion

To summarise we have demonstrated the following:

- The contrast of a band-pass noise carrier has little effect on CM detection beyond around five to six times detection threshold (Experiment 1).
- CM detection generally improves at larger ratios of carrier to envelope spatial frequency. There is no fixed relationship between the spatial frequency of mechanisms sensitive to luminance (first-stage filters) and those sensitive to contrast (second-stage filters). Generally CM detection exhibits *scale invariance* (Experiment 2).
- Side-band structure alone cannot account for detection of CM in noise carriers, even when the contrast of the carrier is high (Experiment 2).
- For low frequency oriented carriers, CM detection is better when carrier and envelope are perpendicular. At higher frequencies all carrier orientations produce similar performance (Experiments 2 and 3).
- Spurious contrast structure in noise carriers can affect CM detection by acting as a mask or contrast pedestal when the spatial frequency of the carrier approaches that of the envelope, and when the boundaries of the orientation cut-off for the noise approach the envelope orientation. Otherwise it does not greatly affect performance (Experiment 3).
- The effect of a noise mask on CM detection is tuned for orientation and spatial frequency. Spatial frequency tuning is relatively narrow-band (half-height at half-width of around 1 octave) as is orientation tuning for horizontal and vertical carriers (half-height at half-width of around 15–30°) (Experiment 4).

We now expand some of these points and discuss their implications for existing models of second-order structure detection.

7.1. No fixed relationship between the spatial frequency of first- and second-stage filters

Experiment 2 describes a steady reduction in CM thresholds for a fixed modulation frequency with increasing carrier spatial frequency. This is consistent with the data reported by Jamar and Koenderink (1985). It is however in contradiction to the results of Sutter et al. (1995) who report a deterioration of CM detection at the highest ratios of carrier to envelope spatial frequency they tested (32:1). They interpret this as evidence for *band-pass* sensitivity of the first-stage filters. Although the deterioration they report is statistically significant, it is small and based on only two data points. For the two subjects presented (in the only condition where the presence of band-pass carrier tuning can be assessed) one subject shows a rise of 14% in CM thresholds, and the other 5%. In this study, we extended the relative frequency range and tested up to a 45:1 ratio of carrier to envelope spatial frequency, using a carrier frequency of 16 cpd. Fig. 5 shows that rather than a deterioration, we report a continued improvement in performance for isotropic, horizontal, and vertical carriers. Fig. 6 illustrates that this trend holds for envelopes at twice the spatial frequency; CM detection exhibits scale invariance over the range tested. Given this, the consistency of our data with findings for CM gratings (Cropper, 1998), our denser sampling of spatial frequency, and that we used more subjects who showed stronger between and within-subject reliability than Sutter et al. (1995), we conclude that this task provides no evidence that CM detection is subserved by linear filters in a fixed spatial frequency relationship with the modulation frequency. We are unable to account for the small decrease in performance reported by Sutter et al. (1995) at the highest carrier frequencies tested.

7.2. No role for side-bands with noise carriers?

With band-pass noise carriers, for the range of relative carrier to envelope spatial frequencies tested, side-band structure was detectable only at levels of contrast modulation exceeding subjects' thresholds. For isotropic carriers and carriers oriented parallel to the envelope, performance is so poor that it seems unlikely that this is a useful cue to the presence of CM. However, for carriers oriented *perpendicular* to the envelope, subjects could reliably detect the presence of side-band structure when ratios of carrier to envelope spatial frequency were less than 2–3 octaves. Thus, these data discount side-band structure as the *sole determinant* of CM detection performance, but do not rule out the possibility (for perpendicular carrier-envelope stimuli at least) that side-band information could be being combined with other (second-order) cues to the presence of local contrast structure. Indeed, the way in which detection thresholds with perpendicular carrier-envelope stimuli dip below thresholds for isotropic carriers (Fig. 5b) suggests that side-band information could be being employed in just this manner.

Why are subjects not able to make better use of side-band structure in our task compared to earlier findings with high contrast carriers (e.g. Jamar et al., 1982)? It seems likely that this is due to the complex phase structure of side-bands resulting from contrast modulation of noise carriers, compared to side-bands originating from modulation of gratings. It is known that the effectiveness of an image as a mask is related to the predictability of its structure compared to the target, a phenomenon recently termed ‘entropy mask- ing’, (Watson, 1997). Similarly one would expect that side-band structure with unpredictable phase structure would be more difficult to detect than the simple side-bands resulting from contrast modulation of gratings (which are punctate in the Fourier domain). This detection will be further hampered by the masking effect of carrier energy present in spatial frequency bands adjacent to the side-bands whose entropy is much higher for noise than for grating carriers. Because of this it seems that noise carriers can be used at higher contrasts than grating carriers without running the risk that CM detection is being performed using side-bands. Experimentally if one wishes to exclude the possibility of side-bands influencing CM detection then one should have subjects discriminate not between CM and unmodulated carriers, but between CM and phase-randomised CM stimuli.

7.3. Estimating first-stage filter tuning using masking

Experiment 4 provided clear evidence that subjects could ignore the influence of a superimposed noise mask on CM detection provided the orientation or spatial frequency of the mask differed sufficiently from the carrier. However, inferring the tuning of a channel directly from an observed pattern of masking is dangerous (for a recent discussion see Nachmias, 1993). For example, it is known that masking of sine-wave grating detection in the presence of simple grating masks leads to underestimation of underlying channel bandwidth. This is because subjects can use channels that are tuned to nearby spatial frequencies or orientations to avoid the influence of noise, a phenomenon termed *off-frequency* (Patterson, 1976; Pelli, 1980; Henning et al., 1981) or *off-orientation* looking (Blake & Holopigian, 1985; Williams, Hess & Demanins, 1998). A task such as ours would also allow subjects to make use of such information. For example, it may be that in order to avoid the influence of masks at 45° on detection of CM of a 90° carrier, that subjects use information from second-stage filters tuned to orientations around 100°, etc. Therefore we make no strong claims about the underlying tuning of first-stage mechanisms from the masking data. We make a more modest claim, that we can reject the hypothesis that first-stage filters are not tuned to either spatial frequency or orientation.

7.4. Orientation relationship between the first- and second-stage filters

For low ratios of carrier to envelope spatial frequencies CM detection is optimal when the carrier and envelope are perpendicular. This trend disappears with increasing carrier spatial frequency. We contend that this is the direct consequence of a mechanism that must segregate luminance and contrast defined structure. When the carrier and envelope are similar (in spatial frequency and orientation), a second-stage filter would not be able to differentiate between first- and second-order information. To avoid this ambiguity, orthogonal first stage filters form the predominant source of input into second stage filters.

As the spatial frequency of the carrier increases, the confusability of luminance and contrast information is greatly reduced and subjects are equally good at detecting contrast modulation irrespective of carrier orientation. This indicates that second-order mechanisms are subserved by first-order mechanisms spanning all orientations. Experiment 4 establishes that individual second-stage filters are subserved by mechanisms tuned to spatial frequency and orientation; this is consistent with observed physiology (Mareschal & Baker, 1998).

7.5. Filter proliferation in two-stage filtering schemes

Experiment 4 provides evidence that the mechanism responsible for detecting contrast modulation is sensitive to the orientation and spatial frequency of the carrier. This is consistent with adaptation work (Langley et al., 1996) and with recent neurophysiology (Mareschal & Baker, 1998). We have also seen that this organisation could confer the second-order visual processing system with ‘multi-purpose’ characteristics, notably the ability to detect both contrast- and texture-defined stimuli. However the disadvantage of such a scheme is that the number of second-order filters required to maintain a detailed mapping from first to second-stage filter orientation and spatial frequency is potentially very large. This problem arises even when one takes into account the fact that second-order mechanisms must be subserved by mechanisms equal or higher in spatial frequency to their own.

Two results from this study indicate a possibility as to how the visual system might avoid this problem. First, in the second part of Experiment 4 we report that masking of CM produces broader tuning with marked asymmetries when the carrier is oblique with respect to the orientation of the contrast modulation. Second, the orientation tuning measured for low frequency carriers in Experiment 3 (e.g. Fig. 8) suggests that parallel carriers are a special case. Taken together these results suggest that second-stage filters could receive narrowly-tuned input only from parallel and perpendicular filters, with oblique orientations being signalled by a small number of more broadly orientationally tuned filters.

There is some indirect evidence bearing on this issue. Wolfson and Landy (1995) have shown that orientation-defined texture edges are most discriminable when texture elements fall either parallel or perpendicular to the defined edge. They have suggested that second-order filters responsible for signalling the presence of a texture edge could be giving greater weight to the input from first-order channels of the same or perpendicular orientation. Dakin, Williams and Hess (1999) proposed that selective connectivity between parallel and perpendicular first- and second-order filters could explain the illusory tilting induced in the Fraser and Zollner illusions, respectively. Additionally, Zanker (1994) has suggested that second-order motion processing could be subserved primarily by filters that are parallel or perpendicular to second-stage filter orientations.

There is another computational reason why parallel and perpendicular inputs could form a 'primary basis' for second-order coding. Recent psychophysical studies of contour detection have indicated that visual contour integration mechanism is tuned for both the orientation and the spatial frequency of contour components (Field, Hayes & Hess, 1993; Dakin & Hess, 1998). A system integrating filter inputs of orientation and spatial frequency similar to it's own would effectively act as an integrator of features whose luminance is correlated with local contour direction. A mechanism integrating perpendicular filter inputs would act as a complementary system integrating features whose luminance was inversely correlated to local contour direction, and there is evidence for sensitivity to contours defined by just such structure (Field et al., 1993).

Such schemes would drastically reduce the number of mechanisms required by a 'filter-rectify-filter' system. If the spatial frequency resolution of the second-order filters were reduced somewhat, one could envisage a system with approximately equal numbers of first- and second-order mechanisms. This is clearly a desirable property of a model making use of finite neural resources.

Acknowledgements

S.C.D. was funded by Canadian MRC grant MT108-18 (to R.F. Hess) and I.M. by FCAR fellowship. Thanks to Rita Demanins and Hok Yean Wong for acting as subjects, and to Robert Hess, Curtis Baker, and Joshua Solomon for their helpful comments on this project.

References

Andrews, D. P. (1965). Perception of contours in the central fovea. *Nature*, *205*, 1218–1220.

Beck, J. (1982). Texture segregation. In J. Beck, *Perceptual organization and representation*. Hillsdale, NJ: Erlbaum.

Blake, R., & Holopigian, K. (1985). Orientation sensitivity in cats and humans assessed by masking. *Vision Research*, *25*, 1459–1467.

Blakemore, C. B., & Carpenter, R. H. S. (1970). Lateral inhibition between orientation detectors in human vision. *Nature*, *228*, 37–39.

Bovik, A., Clark, M., & Geisler, W. (1990). Multi-channel texture analysis using localised spatial filters. *IEEE Transactions on Pattern Analysis and Machine Intelligence*, *12*, 55–73.

Brainard, D. H. (1997). The psychophysics toolbox. *Spatial Vision*, *10*, 433–436.

Burton, G. J. (1973). Evidence for non-linear response processes in the human visual system from measurements on the thresholds of spatial beat frequencies. *Vision Research*, *13*, 1211–1225.

Campbell, F., & Robson, J. (1968). Application of Fourier analysis to the visibility of gratings. *Journal of Physiology*, *197*, 551–566.

Chubb, C., & Sperling, G. (1988). Drift-balanced random stimuli: a general basis for studying non-Fourier motion perception. *Journal of the Optical Society of America A — Optics Image Science*, *5*, 1986–2007.

Cropper, S. J. (1998). Detection of chromatic and luminance contrast modulation by the visual system. *Journal of the Optical Society of America A — Optics Image Science*, *15*, 1969–1986.

Dakin, S. C., & Hess, R. F. (1998). Spatial-frequency tuning of visual contour integration. *Journal of the Optical Society of America*, *15*, 1486–1499.

Dakin, S. C., Williams, C. B., & Hess, R. F. (1999). The interaction of first- and second-order cues to orientation. *Vision Research*, *39*, 2867–2884.

Dannemiller, J. L., & Ver Hoeve, J. N. (1990). Two-dimensional approach to psychophysical orientation tuning. *Journal of the Optical Society of America*, *7*, 141–151.

Daugman, J. G. (1985). Uncertainty relation for resolution in space, spatial-frequency, and orientation optimized by two dimensional cortical filters. *Journal of the Optical Society of America A*, *2*, 1160–1169.

Derrington, A. M., & Badcock, D. R. (1986). Detection of spatial beats: non-linearity or contrast increment detection? *Vision Research*, *26*, 343–348.

Field, D. J., Hayes, A., & Hess, R. F. (1993). Contour integration by the human visual system: evidence for a local association field. *Vision Research*, *33*, 173–193.

Fogel, I., & Sagi, D. (1989). Gabor filters as texture discriminator. *Biological Cybernetics*, *61*, 103–113.

Graham, N, Sutter, A, & Venkatesan (1993). Spatial-frequency and orientation-selectivity of simple and complex channels in region segregation. *Vision Research*, *33*, 1893–1911.

Harvey Jr, L. O., & Doan, V. V. (1990). Visual masking at different polar angles in the two-dimensional Fourier plane. *Journal of the Optical Society of America*, *A7*, 117–127.

Henning, G. B., Hertz, B. G., & Broadbent, D. E. (1975). Some experiments bearing on the hypothesis that the visual system analyses spatial frequency patterns in independent bands of spatial frequency. *Vision Research*, *15*, 887–899.

Henning, G. B., Hertz, B. G., & Hinton, J. L. (1981). Effects of different hypothetical detection mechanisms on the shape of spatial-frequency filters inferred from masking experiments: I. Noise masks. *Journal of the Optical Society of America*, *71*, 574–581.

Jamar, J. H. T., Campagne, J. C., & Koenderink, J. J. (1982). Detectability of amplitude- and frequency-modulation of suprathreshold sine-wave gratings. *Vision Research*, *22*, 407–416.

Jamar, J. H. T., & Koenderink, J. J. (1985). Contrast detection and detection of contrast modulation for noise gratings. *Vision Research*, *25*, 511–521.

Julesz, B. (1981). Textons, the elements of texture perception, and their interactions. *Nature*, *290*, 91–97.

Kovacs, I., & Feher, A. (1997). Non-Fourier information in bandpass noise patterns. *Vision Research*, *37*, 1167–1175.

Langley, K., Fleet, D. J., & Hibbard, P. B. (1996). Linear filtering precedes nonlinear processing in early vision. *Current Biology*, *6*, 891–896.

Ledgeway, T., & Smith, A. T. (1994). Evidence for separate motion-detecting mechanisms for first- and second-order motion in human vision. *Vision Research*, *34*, 2727–2740.

Legge, G. E., & Foley, J. M. (1980). Contrast masking in human vision. *Journal of the Optical Society of America*, *70*, 1458–1471.

Levitt, H. (1970). Transformed up-down methods in psychoacoustics. *Journal of the Acoustical Society of America*, *33*, 467–476.

Malik, J., & Perona, P. (1990). Preattentive texture discrimination with early visual mechanisms. *Journal of the Optical Society of America*, *A7*, 923–932.

Mareschal, I., & Baker, C. L. (1998). A cortical locus for the processing of contrast defined visual stimuli. *Nature Neuroscience*, *1*, 150–154.

Mareschal, I., & Baker, C. L. (1999). Cortical processing of second-order motion. *Visual Neuroscience*, *3*, 527–540.

Marr, D., & Hildreth, E. (1980). Theory of edge detection. *Proceedings of the Royal Society of London*, *B207*, 187–217.

Mostafavi, H., & Sakrison, D. (1976). Structure and properties of a single channel in the human visual system. *Vision Research*, *16*, 957–968.

Nachmias, J. (1993). Masked detection of gratings: the standard model revisited. *Vision Research*, *33*, 1359–1365.

Nachmias, J., & Rogowitz, B. (1983). Masking by spatially modulated gratings. *Vision Research*, *23*, 1621–1630.

Nothdurft, H. C. (1985). Sensitivity for structure gradient in texture discrimination tasks. *Vision Research*, *25*, 1957–1968.

O'Keefe, L. P., & Movshon, J. A. (1998). Processing of first- and second-order motion signals by neurons in area MT of the macaque monkey. *Visual Neuroscience*, *15*, 305–317.

Patterson, R. D. (1976). Auditory filter shapes derived with noise stimuli. *Journal of the Acoustical Society of America*, *59*, 640–654.

Pelli, D. G. (1980). Channel properties revealed by noise masking. *Investigative Ophthalmology and Visual Science Suppl.*, *19*, 44A.

Pelli, D. G. (1997). The VideoToolbox software for visual psychophysics: transforming number into movies. *Spatial Vision*, *10*, 437–442.

Phillips, G., & Wilson, H. (1983). Orientation bandwidths of spatial mechanisms measured by masking. *Journal of the Optical Society of America*, *62*, 226–232.

Ringach, D. L. (1998). Tuning of orientation detectors in human vision. *Vision Research*, *38*, 963–972.

Solomon, J. A., & Watson, A. B. (1995). Spatial and spatial-frequency spreads of masking: measurements and a contrast-gain-control model. *Perception* (*Supplement*), *24*, 37c.

Sutter, A., Beck, J., & Graham, N. (1989). Contrast and spatial variables in texture segregation: testing a simple spatial-frequency channels model. *Perception & Psychophysics*, *46*, 312–332.

Sutter, A., Sperling, G., & Chubb, C. (1995). Measuring the spatial frequency selectivity of second-order texture mechanisms. *Vision Research*, *35*, 915–924.

Thomas, J. P., & Gille, J. (1979). Bandwidths of orientation channels in human vision. *Journal of the Optical Society of America*, *69*, 652–660.

Watson, A. B. (1982). Summation of grating patches indicates many types of detectors at on retinal location. *Vision Research*, *22*, 17–25.

Watson A. B. (1997). Image quality and entropy masking. In *Human Vision*, *Visual Processing*, *and Digital Display VIII*, (pp. 2–12) San Jose, CA: SPIE.

Williams, C. B., Hess, R. F., & Demanins, R. (1998). Orientation tuning estimated by notch-filtered noise masking. *Perception* (*Supplement*), *27*, 80.

Wilson, H., McFarlane, D., & Phillips, G. (1983). Spatial tuning of orientation selective units estimated by oblique masking. *Vision Research*, *23*, 873–882.

Wilson, H. R., Ferrera, P., & Yo, C. (1992). A psychophysically motivated model for two-dimensional motion perception. *Visual Neuroscience*, *9*, 79–97.

Wilson, H. R., & Richards, W. A. (1992). Curvature and separation discrimination and texture boundaries. *Journal of the Optical Society of America*, *A9*, 1653–1662.

Wolfson, S. S., & Landy, M. S. (1995). Discrimination of orientation-defined texture edges. *Vision Research*, *35*, 2863–2877.

Zanker, J. M. (1994). Interactions between primary and secondary mechanisms in human motion perception. *Vision Research*, *34*, 1255–1266.

Zhou, Y. X., & Baker Jr, C. L. (1993). A processing stream in mammalian visual cortex neurons for non-Fourier responses. *Science*, *261*, 98–101.

Zhou, Y. X., & Baker Jr, C. L. (1994). Envelope-responsive neurons in areas 17 and 18 of cat. *Journal of Neurophysiology*, *72*, 2134–2150.

Zhou, Y. X., & Baker Jr, C. L. (1996). Spatial properties of envelope-responsive cells in area 17 and 18 neurons of the cat. *Journal of Neurophysiology*, *75*, 1038–1050.